Available online at www.sciencedirect.com

ScienceDirect

MATTER AND RADIATION AT EXTREMES

Matter and Radiation at Extremes 3 (2018) 219–226

www.journals.elsevier.com/matter-and-radiation-at-extremes

Research Article

High energy and high brightness laser compton backscattering gamma-ray source at IHEP

Guang-Peng An [a,b], Yun-Long Chi [a], Yong-Le Dang [c,e], Guang-Yong Fu [c,e], Bing Guo [c], Yong-Sheng Huang [a,b,*], Chuang-Ye He [c], Xiang-Cheng Kong [a], Xiao-Fei Lan [f], Jia-Cai Li [a,b,**], Fu-Long Liu [c,e], Jin-Shui Shi [d], Xian-Jing Sun [a], Yi Wang [d], Jian-Li Wang [a], Lin Wang [a], Yuan-Yuan Wei [a], Gang Wu [a], Guang-Lei Xu [a], Xiao-Feng Xi [c], Guo-Jun Yang [d], Chun-Lei Zhang [a], Zhuo Zhang [a], Zhi-Peng Zheng [a], Xiao-Ding Zhang [d], Shao-Ping Zhang [a,b]

[a] *Institute of High Energy Physics, Chinese Academy of Sciences, Beijing 100049, China*
[b] *State Key Laboratory of Particle Detection and Electronics, Institute of High Energy Physics, CAS, Beijing 100049, China*
[c] *China Institute of Atomic Energy, Beijing 102413, China*
[d] *Institute of Fluid Physics, China Academy of Engineering Physics, Mianyang 621999, China*
[e] *College of Nuclear Science and Technology, Beijing Normal University, Beijing 100875, China*
[f] *Physics and Space Science College, China West Normal University, Nanchong 637009, China*

Received 17 November 2017; revised 6 January 2018; accepted 28 January 2018
Available online 22 May 2018

Abstract

Based on the LINAC of BEPCII, a high-polarized, high bightness, energy-tunable, monoenergetic laser compton backscattering (LCS) gamma-ray source is under construction at IHEP. The gamma-ray energy range is from 1 MeV to 111 MeV. It is a powerful and hopeful research platform to reveal the underlying physics of the nuclear, the basic particles and the vacuum or to check the exist basic physical models, quantum electrodynamic (QED) theories. In the platform, a 1.064 μm Nd:YAG laser system and a 10.6 μm CO_2 laser system are employed. All the trigger signals to the laser system and the electron control system are from the only reference clock at the very beginning of the LINAC to make sure the temporal synchronization. Two optical transition radiation (OTR) targets and two charged-couple devices (CCD) are used to monitor and to align the electron beam and the laser beam. With the LCS gamma-ray source, it is proposed to experimentally check the gamma-ray calibrations, the photon-nuclear physics, nuclear astrophysics and some basic QED phenomena.

PACS codes: 29.40.-n; 07.85.-m; 29.30.kv

Keywords: laser compton scattering; Calibration; Photon-nuclear physics; Gamma-gamma collider; Nuclear astrophysics; QED; Gamma-gamma scattering; Detection

* Corresponding author. Institute of High Energy Physics, Chinese Academy of Sciences, Beijing 100049, China.
** Corresponding author. Institute of High Energy Physics, Chinese Academy of Sciences, Beijing 100049, China.
E-mail addresses: huangys82@ihep.ac.cn (Y.-S. Huang), lijc@ihep.ac.cn (J.-C. Li).
Peer review under responsibility of Science and Technology Information Center, China Academy of Engineering Physics.

https://doi.org/10.1016/j.mre.2018.01.005

1. Introduction

Based on the 2.5 GeV high-energy electron accelerator, BEPCII at IHEP, a laser compton backscattering (LCS) is under construction to generate high-polarized, high-brightness and monoenergetic gamma rays within a wide energy range, which is a milestone of the experimental study of photon-nuclear physics [1–3] and quantum electrondynamics (QED) phenomena. The LCS gamma-ray source has especially important applications for gamma-ray calibrations, photon-nuclear physics, gamma-gamma collider and so on. For the flash X-ray radiography, the response functions of the image system require series of high-brightness and monoenergetic gamma-ray sources. In a wide energy range, the key data of photon-nuclear physics, such as those of nuclear resonance fluorescence (γ,γ'), (γ,n) reactions [1] and (γ,p) reactions can be acquired and checked experimentally with the LCS gamma-ray sources [4]. In the nuclear astrophysics, the LCS gamma-ray source can help to open the mystery veil of some heavy-elements formations [5]. Also importantly, with two LCS gamma-ray sources, we can establish a gamma-gamma collider, by which one can validate some QED effects experimentally, such as gamma-gamma scattering, electron-positron generation, Delbrüeck scattering [6] and vacuum polarization and so on. In addition, in the near future, with 100 MeV or 100 GeV gamma-gamma collider, one can obtain $\mu(0)$, Higgs particles and can study the related new physics [7].

Based on the important applications, the LCS gamma-ray sources have been appreciated extensively and have been built or planned to build around the world, such as the LADON in Italy [8], the SPARC_LAB Thomson source [9], the LEGS in the NSLS [10], the OK-4 and the HIγS in Duke University [11], the VEPP-4M in Russia, the ELI-NP [12,13], the AIST-LCS and the NewSUBARU [14] in Japan, the SLEGS in Shanghai [2,15] and the LCS-gamma ray source in IHEP. In 1980, Federici and co-workers [8] obtained gamma rays of energy continuously adjustable from 5 MeV to 78 MeV with LCS. The LEGS facility [10] also proposed 300–700 MeV gamma ray beams with 2.5 GeV electron beams or a free electron laser (FEL). At HIγS, the gamma-ray energy reached 225 MeV and the flux exceeded 10^7 photon/s. Several photon-nuclear reactions, such as ^{28}Si $(\overrightarrow{\gamma},\mathrm{p})$ ^{27}Al [16], D $(\overrightarrow{\gamma},\mathrm{p})$n [17,18] were performed by the LCS gamma-ray sources. The SPARC_LAB Thomson source [9] could provide an X-ray energy tunability in the range of 20–500 keV, with measured photon flux of about 10^4. In the proposals of the ELI-NP-GBS (gamma beam system) [12,13], high intensity X-/γ- ray beams in the energy range of 1–20 MeV will be obtained with an electron beam energy tunable from 75 MeV to 750 MeV. The proposed flux can reach 10^9 /s. Recently, a 51.7 keV LCS X-ray with flux of 10^{6-7} /pulse was achieved in Tsinghua University, named Tsinghua Thomson scattering X-ray source (TTX). Xi'an Gamma-ray Light Source (XGLS) has been proposed to obtain a 3 MeV gamma ray beam with a 400 MeV electron beam. SLEGS is planned to generate gamma-ray in the energy range of 2–20 MeV and 300–500 MeV, with the flux of 10^{5-7} photon/s (low energy) and 6×10^6 photon/s (high energy) at SSRF. Besides of conventional accelerators, the laser-plasma acceleration can also be used to generate Compton gamma-ray [19,20]. For the Thomson scattering of a high intensity laser pulse from electrons, it is valuable to improve the scattering gamma-ray yield with proper laser chirping [21]. To make the duration of the laser pulse roughly equal to $2Z_R/c$ with Z_R, i.e., the Rayleigh length, it is the optimal case for the diffracting laser pulse. Another interesting way to increase the photon yield of the source is to use plasma channel [19].

From 2012, based on the high energy electron beam at BEPCII, the LCS gamma-ray source in the energy range of 1–100 MeV, with the flux of 10^{4-5} was proposed. Different from the collision between the laser pulse with the cyclotron-electron beam, there is no need to worry about the quality of the electron beam after LCS. Therefore, we planned to employ 10 ps ultra-intense laser pulse to increase the gamma-ray flux to 10^8/pulse.

Although three big LCS facilities have been proposed in China, they still cannot satisfy the large demand for high-brightness polarized gamma-ray sources. It is absolutely necessary to push the progress of the LCS gamma-ray source.

2. LCS gamma-ray source based on BEPCII at IHEP

2.1. Parameters of the electron beam and the laser systems

At IHEP of CAS, the linac accelerator can supply electron beams of 10 ps and 2 nC in the energy range of 0.2–2.5 GeV. In the first stage, the conventional thermionic cathode gun is still used. A nanosecond Nd:YAG laser system is employed. The parameters of the electron beam and the laser system are shown in Table 1. λ and ω_0 stand for the wavelength of the laser, the diameter of the saddle of the laser pulse in the interaction region, respectively. $\sigma_{x,y}$ is the size of the electron beam in the interaction region, $\varepsilon_{x,y}$ is the normalized emittance of the electron beam.

It is known that there is an excellent approximation of the gamma-ray energy from the LCS [8]:

$$E_\gamma = \frac{x}{1+x+z}E_e, \tag{1}$$

where $x = \frac{4E_eE_l}{(m_ec^2)^2}$, $z = \theta^2\gamma^2$, $\gamma = \frac{E_e}{m_ec^2}$, $E_l = 2\hbar\pi c/\lambda$ is the energy of a single photon, θ is the angle between the emitted gamma and the electron. To avoid the pair production, the optimum value of x is about 4.8. With Eq. (1) and Table 1, the

Table 1
Parameters of electron beams and laser pulses.

Electron beams at E2 line		Nd:YAG laser system	
Energy (GeV)	0.2–2.5	λ (nm)	1064
Duration (ps)	10	Duration (ns)	8–10
Charge (nC)	1–2	E_l (J)	2
$\sigma_{x,y}$ (mm)	1.2	ω_0 (mm)	2.4
$\varepsilon_{x,y}$ (mm·mrad)	338 (370)		
Frequency (Hz)	12.5	Frequency (Hz)	12.5

Table 2
Parameters of the electron injector using the photocathode rf gun.

Initial charge (nC)	1
Charge of the prebuncher (nC)	1
Pulse duration (ps)	10
$\varepsilon_{x,y}$ (mm•mrad)	2.5
Energy (MeV)	59.23
Energy spread (RMS) (%)	0.22

gamma-ray energy range is about 0.7−111 MeV. However, because of the quality of the electron beam and the long pulse duration of the laser pulse, the quality of the gamma ray is not good and the flux is limited.

In the second stage, to improve the quality of the electron beam, a photocathode RF gun will be used to replace the conventional thermionic cathode gun. The parameters of the photocathode rf gun is shown in Table 2.

Besides the photocathode injector, lots of ferromagnets will be renewed to improve the quality of the electron beam. At the same time, the laser system will also be updated to match the electron beam. One YAG laser system and one CO_2 laser system have been designed, as shown by Table 3.

With the ultra-short laser-pulse, the maximum scattered gamma energy is affected by the intensity and is calculated by [22]:

$$E'_{\gamma,\max} = \frac{4\gamma^2 n}{1 + nx + z + a_0^2/2} E_1, \tag{2}$$

for $x \ll 1$, where n is the harmonic number, $a_0 = \frac{eE}{m_e \omega_0 c}$ is the normalized laser field. $n > 1$ corresponds to the nonlinear Compton scattering. As shown by Seipt and coworkers [22], in order to obtain narrowband X- and gamma ray sources, one should explore the compensation which depends on the energy spread and emittance of the electron beam and also the laser focusing.

With the above formulation, the gamma ray energy range is obtained and is shown in Fig. 1.

2.2. The photon flux and energy spectrum

With the parameters of electron beams and laser pulses, the photon flux and energy spectrum have been calculated by the simulation code CAIN [23]. Fig. 2 shows that the gamma-ray energy spectrum of the LCS source employing the 10 ps YAG laser system. It is found that the total photon flux is about 3.68×10^8/pulse. If we count them from 90 MeV to the maximum energy, the flux is larger than 5×10^7/pulse, i.e., 6×10^8/s.

Table 3
Parameters of two laser systems in the second stage.

	Nd:YAG laser system	CO_2 laser system
Energy (J)	0.5	1
Duration (ps)	5−12	180
λ (μm)	1.0	10.8
Frequency (Hz)	12.5	12.5

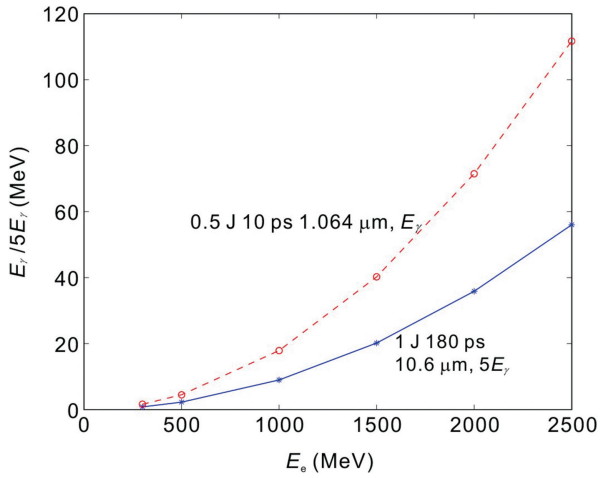

Fig. 1. The gamma-ray energy of the LCS source ranges from 1.6 MeV to 112 MeV corresponding to the Nd:YAG laser, and ranges from 0.16 MeV to 11 MeV corresponding to the CO_2 laser.

For the CO_2 laser system, we also did simulations. As an example, Fig. 3 shows the gamma-ray energy spectrum of the LCS source using the CO_2 laser system shown in Table 3. The total photon flux is about 5.45×10^8/pulse. The photon flux in the energy range [9, 11.5] MeV is also above 1×10^8/pulse, i.e., 1×10^9/s. In the first stage, the simulations also were done and proved the photon flux is about 10^3/pulse, i.e., 10^{4-5}/s. However, in the second stage, since the short-pulse laser system are employed, the photon number density increases significantly. Therefore, with simulation results, the gamma flux can reach 10^{8-9}/s as designed.

2.3. The temporal synchronizing system

In our scheme of LCS gamma-ray source, the head-on collision between the electron beam and the laser pulse is

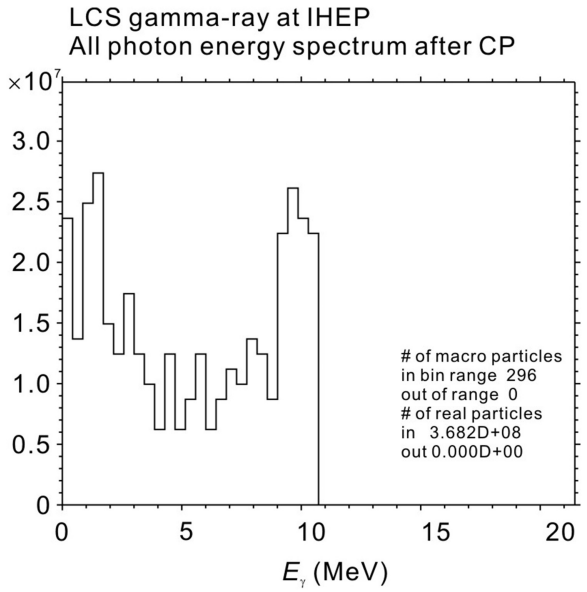

Fig. 2. The gamma-ray energy spectrum of the LCS source with the YAG laser system: 0.5 J and 10 ps. The total photon flux can reach about 3.68×10^8/pulse.

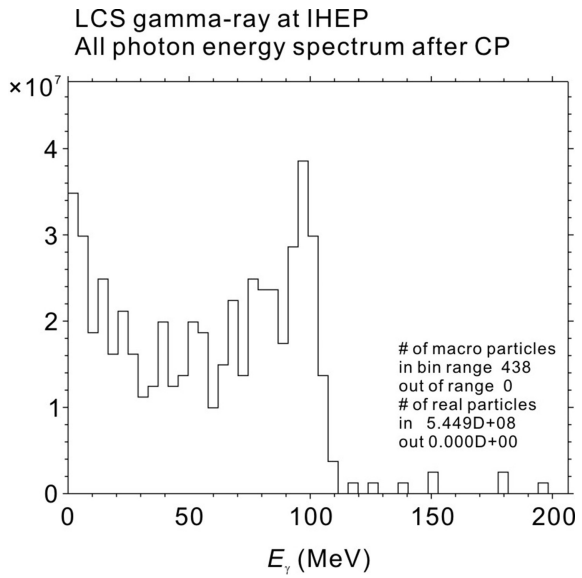

Fig. 3. The gamma-ray energy spectrum of the LCS source with the CO_2 laser system: 1 J and 180 ps. The total photon flux can reach about 5.45×10^8/pulse.

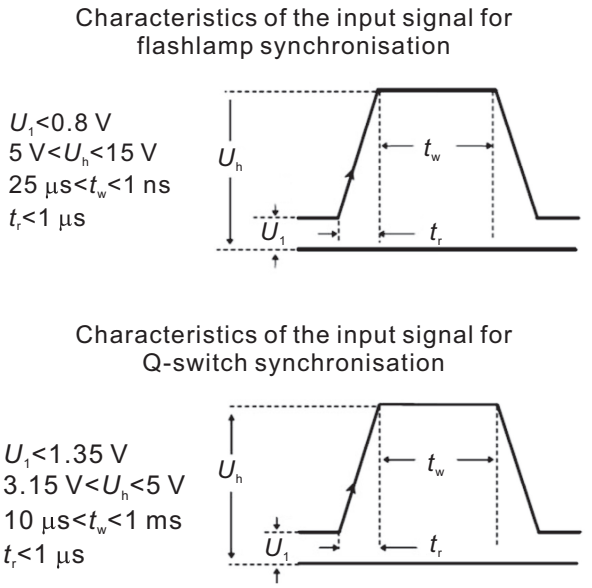

Fig. 5. The required trigger signal of the flashlamp and Q-Switch of the Nd:YAG laser system.

placed in a 100 cm vacuum channel whose inside and outside diameters are 36 mm and 41.5 mm, respectively.

Here, we take the first stage of our LCS system to describe the design of the temporal synchronizing system, which is shown by Fig. 4. The frequency of the trigger signal from the clock is 12.5 Hz. Therefore, the time interval between two pulses is 80 ms. All the trigger signals are delayed a fixed time, t_0. Since the flashlamp needs to be triggered by the previous trigger pulse to ensure the quality of output laser pulse, $t_{FL} = 80\ \text{ms} - 385\ \mu\text{s} + t_0 - 40\ \text{ns} + 1960\ \text{ns}$, where 385 μs is the time interval between the two trigger signals of the flashlamp and the Q-Switch of the laser system. t_{FL} is obtained by a DG535 between the fanout and the flashlamp of the laser system. 40 ns is the time interval between the trigger signal of the Q-Switch and the output laser pulse. The trigger signals of the flashlamp and the Q-Switch are shown in Fig. 5.

After the trigger signal of the electron gun, the electron beam reaches the vacuum chamber of the head-on collision at about 1960 ns. The Q-Switch of the laser system is triggered by the second pulse from the clock. Therefore, to ensure the temporal synchronizing of the laser pulse and the electron beam, $t_Q = t_0 + 1920$ ns.

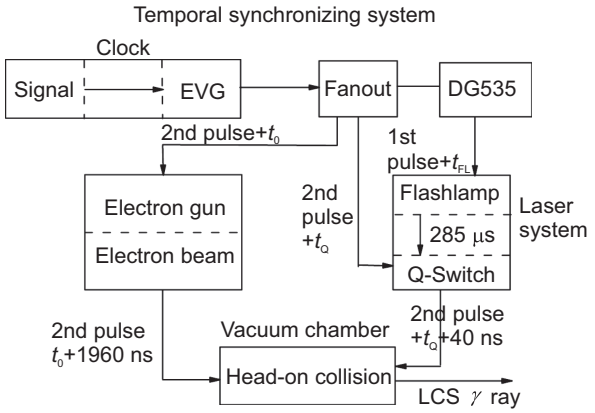

Fig. 4. The temporal synchronizing system of the LCS gamma-ray source. All the trigger signals come from the only one clock.

In this synchronizing system, the time jitter between the electron beam and the laser pulse comes from four items. First, the time jitter of the delayed signal from the fanout to trigger the electron gun, is defined as Δt_{p+t_0}. The second one is the time jitter from the input signal of the electron gun to the colliding vacuum chamber, Δt_{es}. The third is the time jitter of the delayed signal from the fanout to trigger the Q-Switch of the laser system, $\Delta t_{p+t_0+1920\ \text{ns}}$. The last one is the time jitter from the trigger signal of the Q-Switch to the output laser pulse, Δt_Q. The time jitter between the input signals of the flashlamp and the Q-Switch is smaller than 1 μs and just affects the quality of the output laser system tightly. Therefore, in order to guarantee the head-on collision between the electron beam and the laser pulse in the vacuum chamber, it is required that

$$\Delta t = \Delta t_{p+t_0} + \Delta t_{es} + \Delta t_{p+t_0+1920\ \text{ns}} + \Delta t_Q < 0.5\ \text{ns}, \quad (3)$$

The measurement result is $\Delta t < 100$ ps in the first stage.

2.4. The space synchronizing system

At the interaction point, the horizontal cross-section of the electron beam should be contained in that of the laser pulse. Therefore, first, the central axis of the electron beam and the laser pulse should be aligned. The synchronizing system is shown in Fig. 6. To adjust conveniently, we align the He–Ne laser pulse and the main laser pulse first. Then, we aim the electron beam at the He–Ne laser pulse at two points along the vacuum chamber by the imaging system, which contains two optical transition radiation (OTR) targets and two charged-couple devices (CCDs). In front of the collision

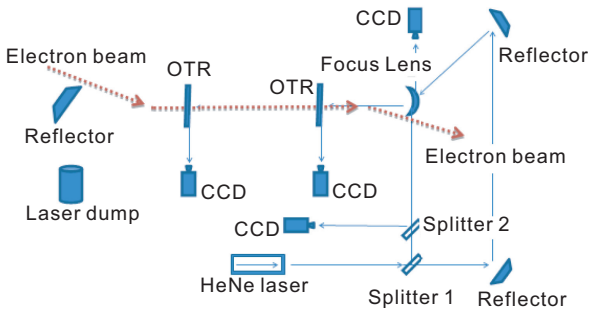

Fig. 6. The space synchronizing system of the electron beam and the laser pulse.

region, beam position monitors (BPMs) are used. Besides the alignment, one needs also to optimize the electron focusing cross-section. The CCD after the beam splitter 2 can help to proofread the coaxiality of the main laser pulse and the He–Ne laser.

The space jitters of the electron beam and the laser pulse are unavoidable. All the light paths from the laser system to the vacuum chamber lie in a vacuum pipeline to avoid air movement and temperature shift. Relatively, the space jitter of the laser pulse is easy to control. Therefore, the diameter of the waist of laser pulse in the colliding region is designed to equal to that of the electron beam plus the jitter.

2.5. The schematic design of the LCS gamma-ray source

Considering the electron-beam line, the laser system, the synchronizing system, the interaction region, the collimator and the gamma-ray detector, the schematic design of the LCS gamma-ray source is shown in Fig. 7.

After the head-on collision between the electron beam and the laser pulse, the gamma rays are emitted in the direction of the electron beam. For high energy (larger than 10 MeV) gamma-ray, the vacuum pipe needs to avoid the gamma-ray burst (GRB) in the air. The collimator is used to shield the low-energy gamma and to decrease the energy spread of the gamma-rays on the detectors. After collision, the electron beam is defected by the magnetic field, E2B, and then goes to a Faraday cup and dump.

For the range between the electron beam line and the laser system, and that between the beam line and the detection system, the radiation shielding and protection have been considered and designed carefully. The shielding structure is 2.1 m thick heavy-metal concrete wall.

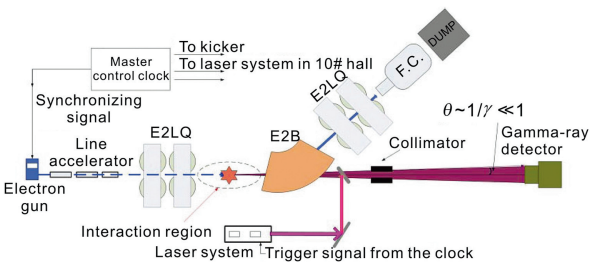

Fig. 7. The schematic design of the LCS gamma-ray source.

2.6. The gamma-ray detectors

The energy range of our LCS gamma-ray source is from 0.1 MeV to 112 MeV. Any single detector cannot cover the large range with acceptable energy resolutions. The range is divided into three subranges: [0.1, 10] MeV, [10, 20] MeV and [20, 112] MeV.

HPGe detectors are designed to detect the gamma rays in the energy range of [0.1, 10] MeV. The resolution is 1.8 keV@1332 keV. The energy efficiency is 70%–100%. To detect the LCS gamma rays, a large range HPGe detector is needed. To detect the gamma-rays from the decay products of the photon-nuclear reactions, the well-type HPGe detector is needed to obtain 100% efficiency. For low-yield transmutation products, one can use a big-volume HPGe detector assisted by a well-type HPGe.

If the gamma-ray energy is larger than 10 MeV, HPGe detector is not proper. In the energy range of [10,20] MeV, $LaBr_3(Ce)$ detectors are designed. The energy resolution is about 2%–3% and is smaller than that of NaI(Tl) detector (about 6%–7%). No matter HPGe or $LaBr_3(Ce)$, the BGO anti-Compton encloser should be used to decrease the background from Compton scattering.

In the first stage, for higher energy gamma rays, we choose the CsI detector in the BES electromagnetic calorimeter (BESEMC), which has been calibrated from 300 MeV to 2 GeV. The energy revolution is about 2%–3%. Another possible solution is the Cherenkov detection [24].

For the calibration of the gamma-ray detectors, the radioactive isotopes and (p,γ) reactions are shown in Table 4.

3. The possible applications of the LCS gamma-ray source based on BEPCII at IHEP

Since the LCS gamma-ray source is highly-polarized, high-brightness, quasi-monoenergetic and energy-tunable, it can be used for gamma-ray calibration, photon-nuclear physics and basic experimental study of the QED phenomena and so on.

3.1. Gamma-ray calibration

Gamma-ray calibration is basic and significant, especially for the flash X-ray radiography of high-energy density physics process and the applications of high-energy cyclotron electron-positron collider (CEPC) synchrotron radiations.

Table 4
The gamma-ray sources for calibration.

Source	Gamma-ray energy (MeV)
^{99}Tc	0.141
^{137}Cs	0.662
^{60}Co	1.13/1.33
^{214}Bi	1.76
^{208}Th	2.62
^{11}B (d,n-γ)^{12}C	4.4/15.1
^{13}C (p,γ)^{14}N	9.17
^{7}Li (p,γ)^{8}Be	17.6

In the flash X-ray radiography of high-energy-density physics process, the projection imaging with the transmitted X-ray can be used to deduce the geometry and the density of the rapidly moving condensed matter. The gamma-ray absorption coefficient, radiation flux and the transforming factor of the exposure of matter depend on gamma energy. Therefore, in the inversion calculations, the response function of the monoenergetic gamma-ray changes with gamma energy and affects the deduction precision directly. With the monoenergetic LCS gamma-ray, the response function of the X-ray radiography system can be achieved easily and precisely.

The energy of the X-ray/gamma-ray from the CEPC synchrotron radiation is from eV to hundreds of MeV. The highest central intensity point is $E_\gamma \approx 326$ keV. Therefore, for the wide application of the synchrotron radiation, the detections must be calibrated precisely by the LCS gamma-ray source.

3.2. Photon-nuclear physics

Because of LCS gamma-ray sources, the photon-nuclear experimental study attracts more and more attentions, in the fields as transmutation induced by LCS gamma-rays [25–27], nuclear astrophysics [28], nuclear resonance fluorescence, photofission of heavy nucleus, giant dipole resonance (GDR), quasi-deuteron effect of nucleus, symmetry breaking and parity measurement and so on [1–3].

3.2.1. Transmutation of long-lived radioisotopes

The reprocessing of the long-lived radioisotopes from nuclear reactors is still challenging, although the accelerator-driven system (ADS) and fast reactors have obtained great progress now. For example, ^{135}Cs is hard to process with neutron beams. In the fission products, lots of ^{134}Cs and ^{133}Cs transform to ^{135}Cs through neutron-capture reactions with large cross-sections.

The (γ, n) reactions induced by the LCS gamma-ray sources are accepted as an effective complementary method to the neutron-capture way. For example, ^{135}Cs can be transmuted to be ^{134}Cs or ^{133}Cs by γ rays [26,27].

3.2.2. Transmutation of heavy-nucleus ^{197}Au

The energy range of the gamma-ray needed in this experiment is [6, 20] MeV. We can take the ^{197}Au $(\gamma, n)^{196}$Au as the benchmark reaction. The LCS gamma-rays are collimated and then are incident on the target through a hole of the target chamber. An HPGe detector is behind the target and detects the rest gamma rays.

The cross section is shown by Fig. 8 and reaches the maximum at $E_\gamma \approx 14$ MeV. The half-life of ^{196}Au is 6.18 days. The plastic scintillator detector and ^{3}He tuber are used to detect the neutrons in near all 4π solid angle. The plastic scintillator detector can also slow down fast neutrons. The neutron detection is affected by the background and other reactions, such as (n,2n). However, an anti-Compton HPGe spectrometer is used to detect the characteristic spectrum, 355.7 keV gamma-ray from the off-line ^{196}Pt.

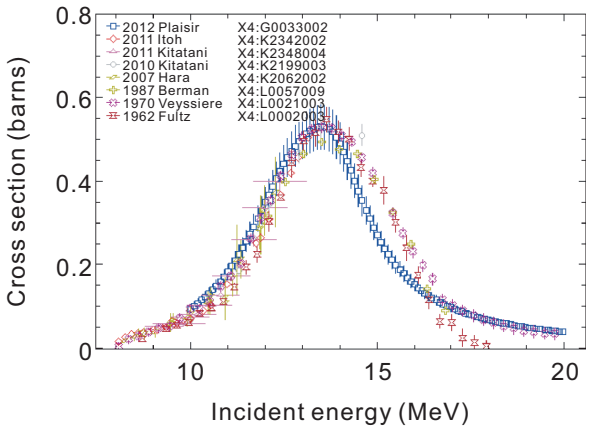

Fig. 8. The cross section of ^{197}Au (γ, n) ^{196}Au *vs* the gamma-ray energy, from the experimental data of NNDC.

With the data of the rest gamma rays, the data of neutrons and the data of the characteristic gamma-rays, one can deduce the cross section of the reaction. Similar with this experiment, a series of photon-nuclear reactions can be studied and be rechecked.

3.2.3. Nuclear astrophysics

Before LCS-gamma source is obtained, the rates of some (γ,n) reactions related with nucleosynthesis have been measured with the bremsstrahlung of the high energy electron accelerators, such as BLBE and S-DALINAC. However, the studies of the (γ,α) and (γ,p) reactions are few and the related data are incomplete.

Although the energy calibration of the gamma-ray can help to improve the experiments, the energy-tunable, quasienergetic LCS gamma source is the best choice for photon–fission reaction study. Recently, the measurements of the (γ, n), (γ, α), (γ, p) reactions of D, ^{9}Be ^{181}Ta, ^{139}La, ^{141}Pr, ^{91,92,94,96}Zr, ^{80}Se, ^{105,106,108}Pd, ^{48}Ca, $^{116-118,120,122,124}$Sn and $^{94-98,100}$Mo have proved the advantages of the LCS gamma-ray sources.

3.3. QED phenomena

The LCS gamma-ray source has high-brightness and is also a good choice to show the vacuum polarization experimentally. Until now, there is no successful experiment to validate vacuum QED effect.

The first application on QED is to check vacuum birefringence. As we know, when a linear polarized light passes through a strong magnetic field or an ultraintense laser pulse, the linear polarization will become elliptic [29,30]. The ellipticity is given by

$$\psi = \pi \frac{L_B}{\lambda} \Delta n_{CM} \sin 2\theta_p, \tag{4}$$

where L_B is the length of the magnetic region or the laser field, λ is the wavelength of the probe wave, $\Delta n_{CM} = n_\perp - n_{||} = k_{CM} B^2$ is the difference of the refractive index, k_{CM} is called Cotton-Mouton constant, and θ_p is the angle between

the light polarization and the magnetic field. If several T magnetic field is used, the effect is so weak to be detected, $k_{CM} \approx 10^{-24}$. If X-ray or gamma-ray interacts with an ultra-intense laser field [31], the effect will be strong enough to be detected. If GeV gamma-ray is used as a probe wave and the intense field of a laser can reach 1000 T, $\psi \propto B^2/\lambda$ will be magnified about $\frac{\text{GeV}}{\text{eV}} \times \left(\frac{1000\ \text{T}}{\text{T}}\right)^2 = 10^9 \times (1000)^2 \approx 10^{15}$ times. However, the detection of the polarization of the X-ray or gamma-ray may be challenging.

If the gamma-ray energy is around 1 MeV, the vacuum light-light scattering and pair production can be checked [32]. The cross section of the vacuum light-light scattering can reach micro-bars [33]. Two gamma-rays collide with each other, the cross section of pair production is about 200 mbar. With the start-to-end simulations, Drebot and coworkers [32] showed the BW process was detectable. We have also done some simulations on the luminosity of the gamma-gamma collision and photon flux with CAIN. Takahashi found the luminosity of the gamma-gamma collision could reach $10^{27}\ \text{cm}^{-2}\cdot\text{s}^{-1}$ with electron parameters: 200 MeV, 2 nC, 1 ps, the normalized emittance, 2.5 μm·mrad, the focusing radius, 2μm; laser parameters: 2 J, 50 Hz, 2 ps, $\lambda = 1.064$ μm, the radius was also 2 μm. In this case, the event rates of $\gamma\gamma \to \gamma\gamma$ and BW process were 5/h and 200/s, respectively. For 135 MeV gamma-gamma collider, high order $\pi(0)$ resonance dependence on polarization can be studied.

4. Conclusion

LCS gamma-ray source combines the advantages of the classical electron accelerator and the ultra-intense laser pulse and can open a new way to experimental study on the underlying physics of the nuclear, basic particles and vacuum. At IHEP, the 1–100 MeV LCS gamma-ray source is under construction. In the near future, photon-nuclear physics, nuclear-astrophysics and some basic QED phenomena will be studied experimentally using that platform.

Conflict of interest

We have no conflict of interest.

Acknowledgments

This work was supported by National Natural Science Foundation of China (11655003), Innovation Project of IHEP (542017IHEPZZBS11820). This work was supported in part by the CAS Center for Excellence in Particle Physics (CCEPP).

References

[1] T. Hayakawa, T. Shizuma, S. Miyamoto, S. Amano, A. Takemoto, et al., Spatial anisotropy of neutrons emitted from the ^{56}Fe (γ, n)^{55} reaction with a linearly polarized γ-ray beam, Phys. Rev. C 93 (4) (2016) 044313, https://doi.org/10.1103/PhysRevC.93.044313.

[2] Q. Pan, X. Wang, J. Chen, W. Guo, G. Fan, et al., Shanghai laser electron γ source(slegs), Nucl. Phys. Rev. 25 (2008) 129–134, https://doi.org/10.11804/NuclPhysRev.25.02.129.

[3] V.G. Nedorezov, Experiments with compton back scattered γ beams on graal collaboration results, Phys. Part. Nucl. 43 (3) (2012) 326–347, https://doi.org/10.1134/S1063779612030057.

[4] S. Gales, D. L. Balabanski, F. Negoita, O. Tesileanu, C.A. Ur, et al., New frontiers in nuclear physics with high-power lasers and brilliant monochromatic gamma beams, Phys. Scripta 91 (9) 093004.

[5] M. Arnould, S. Goriely, The p-process of stellar nucleosynthesis: astrophysics and nuclear physics status, Phys. Rep. 384 (1) (2003) 1–84, https://doi.org/10.1016/S0370-1573(03) 00242–4.

[6] J.K. Koga, T. Hayakawa, Possible precise measurement of delbrück scattering using polarized photon beams, Phys. Rev. Lett. 118 (20) (2017) 204801, https://doi.org/10.1103/PhysRevLett.118.204801.

[7] W. Leemans, W. Chou, M. Uesaka, γ-γ collider, ICFA Beam Dynamics Newsletter 56 (2011) 27.

[8] L. Federici, G. Giordano, G. Matone, G. Pasquariello, P.G. Picozza, et al., Backward compton scattering of laser light against high-energy electrons: the ladon photon beam at frascati, Il Nuovo Cimento 59 (2) (1980) 247–256, https://doi.org/10.1007/BF02721314.

[9] C. Vaccarezza, D. Alesini, M. Anania, A. Bacci, A. Biagioni, et al., The sparc_lab thomson source, Nucl. Instrum. Methods Phys. Res. Sect. A Accel. Spectrom. Detect. Assoc. Equip. 829 (Supplement C) (2016) 237–242, https://doi.org/10.1016/j.nima.2016.01.089, 2nd European Advanced Accelerator Concepts Workshop - EAAC 2015.

[10] A.M. Sandorfi, M.J. LeVine, C.E. Thorn, G. Giordano, G. Matone, et al., High energy γ ray beams from compton backscattered laser light, IEEE Trans. Nucl. Sci. 30 (4) (1983) 3083–3087, https://doi.org/10.1109/TNS.1983.4336577.

[11] V.N. Litvinenko, B. Burnham, M. Emamian, N. Hower, J.M.J. Madey, et al., Gamma-ray production in a storage ring free-electron laser, Phys. Rev. Lett. 78 (24) (1997) 4569–4572, https://doi.org/10.1103/PhysRevLett.78.4569.

[12] Serafini, L., Alesini, D., Bacci, N., Bliss, N., Cassou, K., et al., High Intensity x/γ Photon Beams for Nuclear Physics and Photonicsdoi: 10.1051/epjconf/201611705002.

[13] V. Petrillo, A. Bacci, R.B.A. Zinati, I. Chaikovska, C. Curatolo, et al., Photon flux and spectrum of γ-rays compton sources, Nucl. Instrum. Methods Phys. Res. Sect. A Accel. Spectrom. Detect. Assoc. Equip. 693 (Supplement C) (2012) 109–116, https://doi.org/10.1016/j.nima.2012.07.015.

[14] S. Miyamoto, Y. Asano, S. Amano, D. Li, K. Imasaki, et al., Laser compton back-scattering γ-ray beamline on newsubaru, Radiat. Meas. 41 (Supplement 2) (2006) S179–S185, https://doi.org/10.1016/j.radmeas.2007.01.013. The 3rd International Workshop on Radiation Safety at Synchrotron Radiation Sources.

[15] W. Guo, W. Xu, J. Chen, Y. Ma, X. Cai, et al., A high intensity beam line of gamma-rays up to 22mev energy based on compton backscattering, Nucl. Instrum. Methods Phys. Res. Sect. A Accel. Spectrom. Detect. Assoc. Equip. 578 (3) (2007) 457–462, https://doi.org/10.1016/j.nima.2007.05.322.

[16] A.D. Rosa, G. Inglima, M. Sandoli, D. Prosperi, G. Giordano, et al., Multipole mixture contribution to the ^{28}Si giant-resonance excitation, Lett. al Nuovo Cimento 40 (13) (1984) 401–406, https://doi.org/10.1007/BF02739653.

[17] M.W. Ahmed, M.A. Blackston, B.A. Perdue, W. Tornow, H.R. Weller, et al., Near-threshold deuteron photodisintegration: an indirect determination of the gerasimov-drell-hearn sum rule and forward spin polarizability (γ_0) for the deuteron at low energies, Phys. Rev. C 77 (4) (2008) 044005, https://doi.org/10.1103/PhysRevC.77.044005.

[18] M.A. Blackston, M.W. Ahmed, B.A. Perdue, H.R. Weller, B. Bewer, et al., First observation of the splittings of the $e1$ p-wave amplitudes in low energy deuteron photodisintegration and its implications for the gerasimov-drell-hearn sum rule integrand, Phys. Rev. C 78 (3) (2008) 034003, https://doi.org/10.1103/PhysRevC.78.034003.

[19] S. G. Rykovanov, C. G. R. Geddes, J.-L. Vay, C. B. Schroeder, E. Esarey, et al., Quasi-monoenergetic femtosecond photon sources from thomson scattering using laser plasma accelerators and plasma channels, J. Phys. B Atomic. Mol. Optical. Phys. 47 (23) 234013.

[20] C.G. Geddes, S. Rykovanov, N.H. Matlis, S. Steinke, J.-L. V, et al., Compact quasi-monoenergetic photon sources from laser-plasma accelerators for nuclear detection and characterization, Nucl. Instrum. Methods Phys. Res. Sect. B Beam Interact. Mater. Atoms 350 (Supplement C) (2015) 116−121, https://doi.org/10.1016/j.nimb.2015.01.013.

[21] S.G. Rykovanov, C.G.R. Geddes, C.B. Schroeder, E. Esarey, W.P. Leemans, Controlling the spectral shape of nonlinear thomson scattering with proper laser chirping, Phys. Rev. Accel. Beams. 19 (2016) 030701, https://doi.org/10.1103/PhysRevAccelBeams.19.030701.

[22] D. Seipt, S.G. Rykovanov, A. Surzhykov, S. Fritzsche, Narrowband inverse compton scattering x-ray sources at high laser intensities, Phys Rev A 91 (3) (2015) 033402, https://doi.org/10.1103/PhysRevA.91.033402.

[23] K. Yokoya, User's Manual of Cain, Version 2.42 1, 2011, p. 1.

[24] P. Rose, A. Erickson, Calibration of cherenkov detectors for monoenergetic photon imaging in active interrogation applications, Nucl. Instrum. Methods Phys. Res. Sect. A Accel. Spectrom. Detect. Assoc. Equip. 799 (Supplement C) (2015) 99−104, https://doi.org/10.1016/j.nima.2015.07.065.

[25] W.S. Yang, Y. Kim, R.N. Hill, T.A. Taiwo, H.S. Khalil, Long-lived fission product transmutation studies, Nucl. Sci. Eng. 146 (2004) 291−318, https://doi.org/10.13182/NSE04-A2411.

[26] Z. Zhu, W. Luo, Z. Li, Y. Song, X. Wang, X. Wang, G. Fan, Phototransmutation of long-lived nuclear waste 135cs by intense compton gamma-ray source, Ann. Nucl. Energy 89 (Supplement C) (2016) 109−114, https://doi.org/10.1016/j.anucene.2015.11.017.

[27] D.Z. Li, K.Z. Imasaki, K. Horikawa, S.J. Miyamoto, S. Amano, et al., Iodine transmutation through laser compton scattering gamma rays, J. Nucl. Sci. Technol. 46 (8) (2009) 831−835, https://doi.org/10.1080/18811248.2007.9711592.

[28] T. Rauscher, N. Dauphas, I. Dillmann, C. Frhlich, Z. Flp, et al., Constraining the astrophysical origin of the p-nuclei through nuclear physics and meteoritic data, Rep. Prog. Phys. 76 (8) (2013) 066201, https://doi.org/10.1088/0034-4885/76/6/066201.

[29] P. Berceau, M. Fouché, R. Battesti, C. Rizzo, Magnetic linear birefringence measurements using pulsed fields, Phys. Rev. A 85 (1) (2012) 013837, https://doi.org/10.1103/PhysRevA.85.013837.

[30] A. Cadène, D. Sordes, P. Berceau, M. Fouché, R. Battesti, et al., Faraday and cotton-mouton effects of helium at λ=1064 nm, Phys. Rev. A 88 (4) (2013) 043815, https://doi.org/10.1103/PhysRevA.88.043815.

[31] S. Bragin, S. Meuren, C.H. Keitel, A. Di Piazza, High-energy vacuum birefringence and dichroism in an ultrastrong laser field, Phys. Rev. Lett. 119 (2017) 250403, https://doi.org/10.1103/PhysRevLett.119.250403.

[32] I. Drebot, D. Micieli, E. Milotti, V. Petrillo, E. Tassi, et al., Matter from light-light scattering via breit-wheeler events produced by two interacting compton sources, Phys. Rev. Accel. Beams. 20 (2017) 043402, https://doi.org/10.1103/PhysRevAccelBeams.20.043402.

[33] K. Homma, K. Matsuura, K. Nakajima, Testing helicity-dependent gamma-gamma scattering in the region of mev, Prog. Theor. Exp. Phys. 2016 (1) (2016) 013C01, https://doi.org/10.1093/ptep/ptv176.